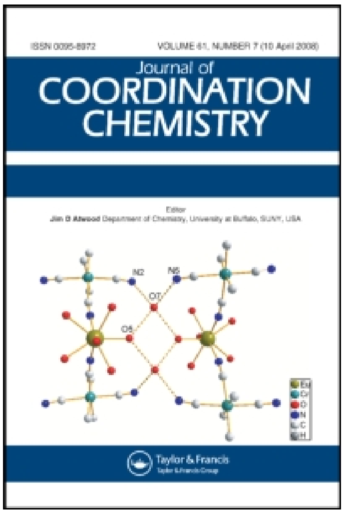

Journal of Coordination Chemistry
Publication details, including instructions for authors and subscription information:
http://www.informaworld.com/smpp/title~content=t713455674

Synthesis, characterization and catalytic oxidation of cyclohexene with molecular oxygen over host (nanopores of zeolite-Y)/guest ($[Ni([R]_2-N_2X_2)]^{2+}$ (R = H, CH_3; X = NH, O, S) nanocatalyst

Masoud Salavati-Niasari[ab]
[a] Institute of Nano Science and Nano Technology, University of Kashan, Kashan, I. R. Iran [b] Faculty of Science, Department of Chemistry, University of Kashan, Kashan, I. R. Iran

To cite this Article Salavati-Niasari, Masoud(2009) 'Synthesis, characterization and catalytic oxidation of cyclohexene with molecular oxygen over host (nanopores of zeolite-Y)/guest ($[Ni([R]_2-N_2X_2)]^{2+}$ (R = H, CH_3; X = NH, O, S) nanocatalyst', Journal of Coordination Chemistry, 62: 6, 980 — 995

To link to this Article: DOI: 10.1080/00958970802322863

URL: http://dx.doi.org/10.1080/00958970802322863

Journal of Coordination Chemistry
Vol. 62, No. 6, 20 March 2009, 980–995

Taylor & Francis
Taylor & Francis Group

Synthesis, characterization and catalytic oxidation of cyclohexene with molecular oxygen over host (nanopores of zeolite-Y)/guest ($[Ni([R]_2\text{-}N_2X_2)]^{2+}$ ($R = H, CH_3$; $X = NH, O, S$) nanocatalyst

MASOUD SALAVATI-NIASARI*†‡

†Institute of Nano Science and Nano Technology, University of Kashan, Kashan,
P. O. Box 87317-51167, I. R. Iran
‡Faculty of Science, Department of Chemistry, University of Kashan, Kashan,
P. O. Box 87317-51167, I. R. Iran

(*Received 27 February 2008; in final form 23 May 2008*)

Nickel(II) complexes of 12-membered macrocyclic ligands with different donating atoms (N_2O_2, N_2S_2 and N_4) in the macrocyclic ring have been encapsulated in the nanocavity of zeolite-Y by the fexible-ligand method. Nickel(II) complexes with macrocyclic ligands were entrapped in the nanocavity of zeolite-Y by a two-step process in the liquid phase: (i) adsorption of precursor ligand; 1,2-di(*o*-aminophenyl-, amino, oxo, thio)ethane, N_2X_2; in the supercages of the Ni(II)–NaY, and (ii) *in situ* condensation of the Ni(II) precursor complex; $[Ni(N_2X_2)]^{2+}$; with glyoxal or biacetyl. The new host–guest nanocatalysts (HGNM), $[Ni([R]_2\text{-}N_2X_2)]^{2+}$–NaY ($R = H, CH_3$; $X = NH, O, S$), have been characterized by FT-IR, DRS and UV–Vis spectroscopic techniques, XRD and elemental analysis, as well as nitrogen adsorption, and were used for oxidation of cyclohexene with molecular oxygen.

Keywords: Nanocomposite material; Host–guest; Oxidation of cyclohexene; Zeolite encapsulation; Nickel(II)

1. Introduction

Heterogenization of metal complexes known to be active in homogeneous catalysis inside of zeolite pores can be achieved via ship-in-the-bottle synthesis. The three-dimensional large pore zeolites X with pore of 7.4 Å are often chosen as a host framework. The size of the zeolite supercages enables synthesis and accommodation of nanosized metal complexes inside those cavities, but their openings do not allow the synthesized complex to diffuse away. When encapsulation of metal complexes is carried out through the flexible ligand method all individual components like the metal ion and ligand can easily pass in and out of the zeolite, but the final coordination complex is too large and rigid to go out once assembled inside. The complex immobilized in this way also acquires new properties. When confined in the zeolite voids, the complex may lose

---

*Email: salavati@kashanu.ac.ir

Journal of Coordination Chemistry
ISSN 0095-8972 print/ISSN 1029-0389 online
DOI: 10.1080/00958970802322863

some of its degrees of freedom or adopt a unique geometry, different than in solution. The surrounding zeolite framework may also affect selectivity of catalytic reactions by influencing transition states of parallel processes [1–21].

The encapsulation (ship-in-a-bottle) approach is convenient because the encapsulated complex, once formed inside the cages of the zeolite, is too large to diffuse out and is not lost into the liquid phase during the reaction. As these composite materials mimic biological enzymes, they are also called "zeozymes" (acronym for zeolite mimics of enzymes). In a general sense, the encapsulated complexes mimic enzyme systems in that the porous inorganic mantle (similar to the protein mantle in enzymes) provides (hopefully) the right steric requirement for the metal complex and imposes certain requirements (based on size and shape) to the access of the active site by the substrate (substrate selectivity). Though many nanoporous materials have been used, the most popular ones have been zeolites Y possessing large cages (1.2 nm diameters) [3–21].

In this article, I report the synthesis and characterization of nickel(II) complexes of a 12-membered macrocyclic ligand, 1,4-diaza,7,10-dioxo,5,6 : 11,12-dibenzo-[*e*, *k*]-cyclododeca-1,3-diene[N_2O_2]ane; $[H]_2$–N_2O_2, 2,3-dimethyl-1,4-diaza,7,10-dioxo,5,6 : 11,12-dibenzo-[*e*, *k*]-cyclododeca-1,3-diene[N_2O_2]ane; $[CH_3]_2$-N_2O_2, 1,4,7,10-tetraaza-5,6 : 11,12-dibenzo-[*e*, *k*]-cyclododeca-1,3-diene[N_4]ane; $[H]_2$–N_4, 2,3-dimethyl-1,4,7,10-tetraaza-5,6 : 11,12-dibenzo-[*e*, *k*]-cyclododeca-1,3-diene[N_4]ane; $[CH_3]_2$–N_4, 1,4-diaza, 7,10-dithia,5,6 : 11,12-dibenzo-[*e*, *k*]-cyclododeca-1,3-diene[N_2S_2]ane; $[H]_2$–N_2S_2 and 2,3-dimethyl-1,4-diaza,7,10-dithia,5,6 : 11,12-dibenzo-[*e*, *k*]-cyclododeca-1,3-diene [N_2S_2]ane; $[CH_3]_2$-N_2S_2; encapsulated within the nanopores of zeolite-Y by the template condensation of glyoxal or biacetyl and precursor complex ($[Ni([R]_2\text{-}N_2X_2)]^{2+}$–NaY, R = H, CH_3; X = NH, O, S) shown in schemes 1 and 2 and used in the oxidation of cyclohexene with molecular oxygen.

2. Experimental

2.1. *Materials*

Safety note – Perchlorate salts of transition metal complexes with organic ligands are often explosive and should be handled with caution.

Cyclohexene was distilled under nitrogen and stored over molecular sieves (4 Å). Cyclohexanone was used as an internal standard for quantitative analysis of the product using gas chromatography. Reference samples of 2-cyclohexene-1-ol and 2-cyclohexene-1-one (Aldrich) were distilled and stored in the refrigerator. NaY with the Si:Al ratio of 2.53 was purchased from Aldrich (Lot No. 67812).

2.2. *Physical measurements*

Diffuse reflectance spectra (DRS) were recorded on a Shimadzu UV/3101 PC spectrophotometer from 1500–200 nm, using MgO as reference. The elemental analysis (carbon, hydrogen and nitrogen) of the materials was obtained from a Carlo ERBA Model EA 1108 analyzer. X-ray diffraction (XRD) patterns were recorded by a Rigaku D-max C III, X-ray diffractometer using Ni-filtered Cu-Kα radiation. Nitrogen adsorption measurements were performed at 77 K using a Coulter Ofeisorb 100CX instrument.

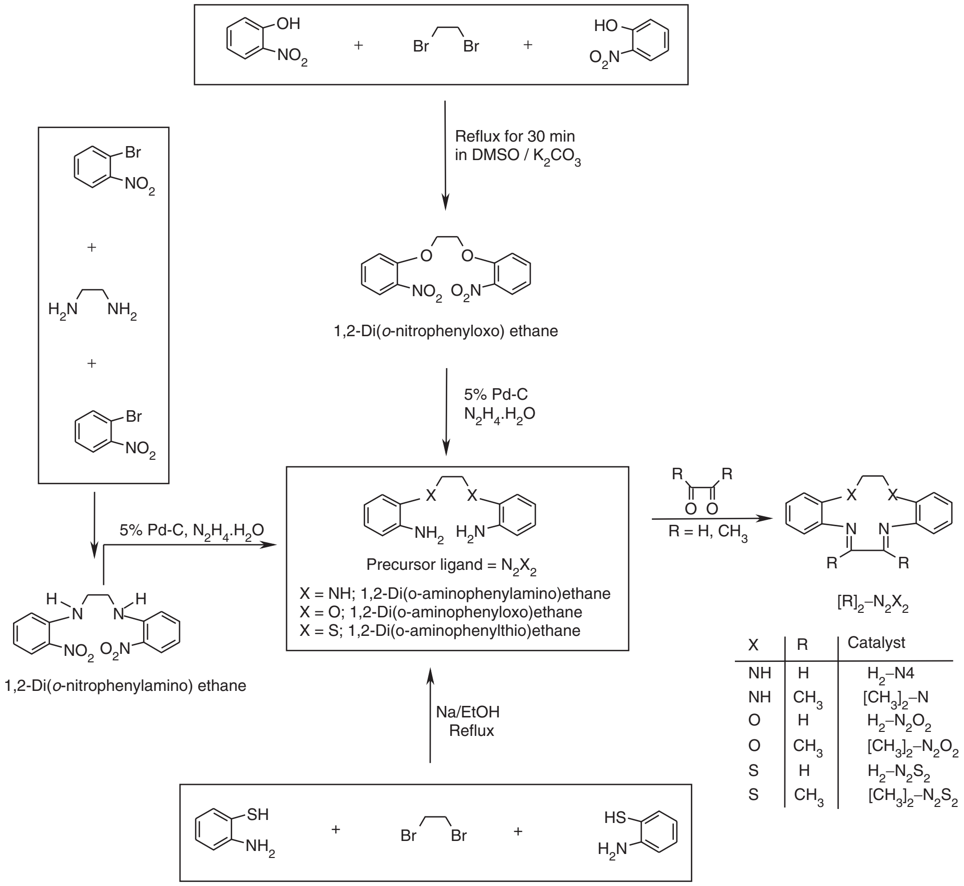

Scheme 1. Reaction mechanism of 12-membered macrocyclic ligands.

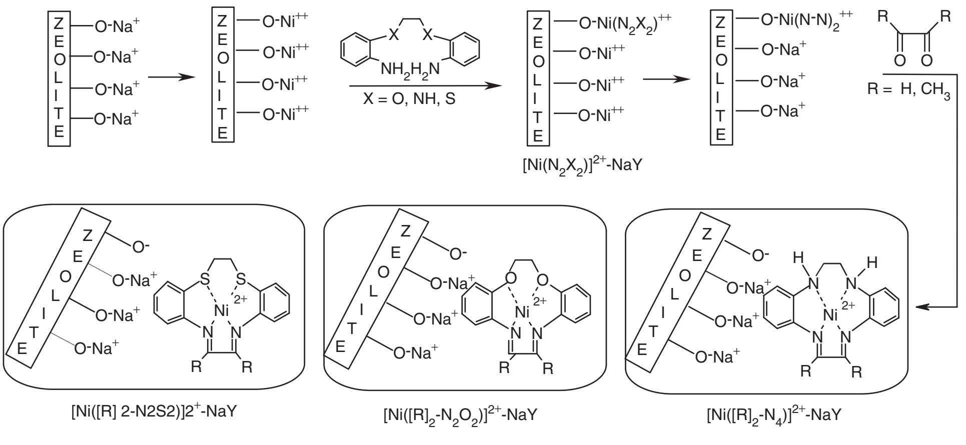

Scheme 2. Encapsulation of 12-membered macrocyclic ligand.

The samples were degassed at 150°C until a vacuum better than 10^{-3} Pa was obtained. Micropore volumes were determined by the *t*-method, a "monolayer equivalent area" was calculated from the micropore volume [22, 23]. ^{1}H-NMR spectra were obtained on a Bruker NMR 400 (400 MHz) spectrophotometer using $CDCl_3$ and $(CD_3)_2SO$ as solvents. FT-IR spectra were recorded on a Shimadzu Varian 4300 spectrophotometer in KBr pellets. Electronic spectra of neat complexes were taken on a Shimadzu UV–Vis scanning spectrometer (Model 2101 PC). The stability of the encapsulated catalyst was checked after the reaction by UV–Vis and possible leaching of the complex was investigated by UV–Vis in the reaction solution after filtration of the zeolite. The amounts of nickel(II) complexes encapsulated in zeolite matrix were determined by elemental analysis and by subtracting the amount of nickel(II) complex left in the solutions after the synthesis of the catalysts as determined by UV–Vis spectroscopy. Atomic absorption spectra (AAS) were recorded on a Perkin–Elmer 4100–1319 spectrophotometer using a flame approach, after acid (HF) dissolution of known amounts of the zeolitic material and SiO_2 was determined by gravimetric analysis. Gas chromatography experiments (GC) were performed with a Shimadzu GC-16A instrument.

2.3. *Synthesis of 1,2-di(o-aminophenyloxo)ethane*

Ortho-nitrophenol (4.78 g) in hot dimethylformamide (5.0 mL) was treated slowly with potassium carbonate (2.39 g). The resulting solution was boiled gently and 1,2-dibromoethane (1.54 mL) was added dropwise with constant stirring for 30 min. The mixture was then refluxed gently for 2 h and concentrated under reduced pressure. On pouring the solution into cold water a granular yellow solid was filtered, washed with dilute aqueous NaOH, dried and recrystallized from glacial acetic acid, m.p. 169°C. ^{1}H-NMR: ($CDCl_3$) δ 8.18 (2H, d), δ 7.35 (2H, m), δ 7.76 (2H, m), δ 7.08 (H, d), δ 4.08 (4H, O–CH_2) (scheme 1). 1,2-Di(*o*-nitrophenyloxo)ethane was heated under a nitrogen atmosphere with 5% Pd–C (0.5 g). $N_2H_4 \cdot H_2O$ (20.0 mL) was added in (5 mL) portions and the mixture refluxed until the solution become colorless (30 min). After filtration to remove the precipitate (if any), the solution was evaporated to dryness and the solid residue recrystallized from hot ethanol under a nitrogen atmosphere. A residue of white plates was obtained. m.p. 131°C. ^{1}H-NMR: ($CDCl_3$) δ 6.35 (2H, d), δ 7.16 (2H, m), δ 6.65 (2H, m), δ 7.08 (2H, d), δ 4.03 (4H, O–CH_2) (scheme 1).

2.4. *Synthesis of 1,2-di(o-aminophenylamino)ethane*

1,2-Di(*o*-nitrophenylamino)ethane was prepared by heating $BrC_6H_4NO_2$ (2.0 g) with 1,2-diaminoethane (0.26 mL). The mixture was stirred rigorously until complete reaction occurred. The heating was then reduced to keep the mass molten for further use. The melt was poured into ethanol (50.0 mL), the solid so obtained was washed with a mixture of diethyl ether (30.0 mL), benzene (30.0 mL) and 1 N NaOMe solution (10 mL) and recrystallized from 1,2-dichloroethane give 1,2-di(*o*-nitrophenylamino)ethane (3.1 g) as bright orange needle-shaped crystals. m.p. 193°C. ^{1}H-NMR: ($CDCl_3$) δ 8.1 (2H, d), δ 7.33 (2H, m), δ 7.75 (2H, m), δ 7.06 (H, d), δ 4.07 (4H, NH–CH_2) (scheme 1).

1,2-Di(*o*-nitrophenylamino)ethane was heated under a nitrogen atmosphere with 5% Pd–C (0.5 g). $N_2H_4 \cdot H_2O$ (20.0 mL) was added in (5 mL) portions and the mixture refluxed until the solution become colorless (30 min). After filtration to remove the precipitate (if any), the solution was evaporated to dryness and the solid residue recrystallized from hot ethanol under a nitrogen atmosphere. A residue of white plates was obtained. M.p. 135°C. ^{1}H-NMR: ($CDCl_3$) δ 6.36 (2H, d), δ 7.15 (2H, m), δ 6.65 (2H, d), δ 6.73 (2H, d), δ 3.04 (4H, m, NH–CH_2) diamine(II) (scheme 1).

2.5. *Synthesis of 1,2-di(o-aminophenylthio)ethane*

This diamine was prepared by heating *o*-$HSC_6H_4NH_2$ (1.09 g) with absolute (99%) ethanol (3 mL) containing sodium (0.201 g). 1,2-Dibromoethane (0.372 mL) in ethanol (1 mL) was then added dropwise with constant stirring to the refluxing solution. The mixture was cooled and poured into water (300 mL). The solid product was filtered, washed with water, dried and recrystallized from ethanol giving a yellowish residue. m.p. 75°C. ^{1}H-NMR: ($CDCl_3$) δ 6.35 (2H, d), δ 7.15 (2H, m), δ 6.63 (2H, m), δ 7.24 (2H, d), δ 2.88 (4H, m, S-CH_2) (scheme 1).

2.6. *Synthesis of macrocyclic ligands ($[R]_2$–N_2X_2, R = H, CH_3; X = NH, O, S)*

1,4-Diaza,7,10-dioxo,5,6 : 11,12-dibenzo-[*e*, *k*]-cyclododeca-1,3-diene[N_2O_2]ane; $[H]_2$–N_2O_2, 2,3-dimethyl-1,4-diaza,7,10-dioxo,5,6 : 11,12-dibenzo-[*e*, *k*]-cyclododeca-1,3-diene[N_2O_2]ane; $[CH_3]_2$–N_2O_2, 1,4,7,10-tetraaza-5,6 : 11,12-dibenzo-[*e*, *k*]-cyclododeca-1,3-diene[N_4]ane; $[H]_2$–N_4, 2,3-dimethyl-1,4,7,10-tetraaza-5,6 : 11,12-dibenzo-[*e*, *k*]-cyclododeca-1,3-diene[N_4]ane; $[CH_3]_2$-N_4, 1,4-diaza,7,10-dithia,5,6 : 11,12-dibenzo-[*e*, *k*]-cyclododeca-1,3-diene[N_2S_2]ane; $[H]_2$–N_2S_2 and 2,3-dimethyl-1,4-diaza,7,10-dithia,5,6 : 11, 12-dibenzo-[*e*, *k*]-cyclododeca-1,3-diene[N_2S_2]ane; $[CH_3]_2$–N_2S_2 were obtained as described. To an ethanol solution (25 mL) of 0.05 mol glyoxal or biacetyl, an ethanol solution (25 mL) of precursor ligand [1, 2-di(*o*-aminophenyloxo)ethane, 1,2-di(*o*-aminophenylamino)ethane, 1,2-di(*o*-aminophenylthio)ethane (0.05 mol)] was added in the presence of a few drops of conc. HCl and the resulting solution boiled under reflux for 8 h. The solution was then concentrated to half its volume under reduced pressure and kept overnight. The white/off-white crystals which formed were filtered, washed with ethanol and dried under vacuum over P_4O_{10}. ^{1}H-NMR, ($CDCl_3$); $[H]_2$–N_4: δ 8.01 (2H, s), 6.93 (2H, d), d 7.14 (2H, m), 6.65 (2H, m), 6.76 (2H, d), 3.12 (4H, NH–CH_2); $[CH_3]_2$–N_4: δ 2.09 (6H, s), 6.92 (2H, d), d 7.13 (2H, m), 6.65 (2H, m), 6.75 (2H, d), 3.11 (4H, NH–CH_2); $[H]_2$–N_2O_2: δ 8.05 (2H, s), 6.92 (2H, d), d 7.12 (2H, m), 6.63 (2H, m), 6.74 (2H, d), 4.13 (4H, O–CH_2); $[CH_3]_2$–N_2O_2: δ 2.13 (6H, s), 6.91 (2H, d), d 7.12 (2H, m), 6.62 (2H, m), 6.73 (2H, d), 4.13 (4H, O–CH_2); $[H_2]$–N_2S_2: δ 7.92 (2H, s), 6.90 (2H, d), d 7.11 (2H, m), 6.60 (2H, m), 6.72 (2H, d), 4.11 (4H, S-CH_2); $[CH_3]_2$–N_2S_2: δ 1.94 (6H, s), 6.90 (2H, d), d 7.10 (2H, m), 6.60 (2H, m), 6.72 (2H, d), 4.10 (4H, S–CH_2) (scheme 1).

2.7. *Preparation of $[Ni([R]_2$–$N_2X_2)](ClO_4)_2$ (R = H, CH_3; X = NH, O, S)*

Nickel(II) sulfate hexahydrate (2.63 g, 0.01 mol) dissolved in ethanol (20 mL) was reacted with an ethanol (20 mL) solution 0.01 mol of 12-membered macrocyclic ligand

($[H]_2$–N_4, $[CH_3]_2$–N_4, $[H]_2$–N_2O_2, $[CH_3]_2$–N_2O_2, $[H]_2$–N_2S_2, $[CH_3]_2$–N_2S_2) by refluxing for 1 h under nitrogen atmosphere. The mixture was heated at reflux for 6 h until a yellow solution resulted. The solution was cooled to room temperature and filtered to remove nickel hydroxide. Excess lithium perchlorate dissolved in methanol was added to the filtrate, and the mixture was kept in the refrigerator until a yellow solid formed. The solids were filtered, washed thoroughly with cold ethanol and dried in vacuum.

2.8. *Preparation of $[Ni(N_2X_2)]^{2+}$–NaY ($X = NH, O, S$)*

An amount of 5.0 g of Na-Y-zeolite was suspended in 300 mL distilled water, which contained nickel(II) nitrate (50 mmol). The mixture was then heated with stirring at 90°C for 24 h. The solid was filtered, washed with hot distilled water until the filtrate was free from any nickel, and dried for 12 h at 150°C in air. The ionic exchange degree was determined by atomic absorption spectrophotometer. To a stirred methanol solution of Ni(II)–NaY (4 g) was uniformly mixed with an excess of 1,2-di(*o*-aminophenyloxo)ethane, 1,2-di(*o*-aminophenylamino)ethane or 1,2-di(*o*-aminophenylthio)ethane ligands ($n_{\text{ligand}}/n_{\text{metal}} = 3$) and sealed into a flask. The complexation was carried out under high vacuum conditions for 24 h at 150°C. Uncomplexed ligands and the complex adsorbed on the exterior surface were removed by Soxhlet extraction with ethanol. The extracted sample was ion-exchanged with 0.1 M NaCl aqueous solution to remove uncoordinated Ni^{2+} ions, followed by washing with deionized water until no Cl^- could be detected with $AgNO_3$ aqueous solution.

2.9. *Preparation of $[Ni([R]_2\text{-}N_2X_2)]^{2+}$–NaY ($R = H, CH_3$; $X = NH, O, S$)*

To a stirred methanol suspension (100 mL) of precursor nanocatalyst ($[Ni(N_2X_2)]^{2+}$–NaY) (2 g) was slowly added glyoxal or biacetyl (under N_2). The mixture was heated under reflux for 24 h until a pale yellow suspension resulted. The solution was filtered and the resulting zeolites were Soxhlet extracted with *N*,*N*′-dimethylformamide (for 4 h) and then with ethanol (for 4 h) to remove unreacted products from amine–carbonyl condensation and any nickel(II) complexes adsorbed onto the surface of the zeolite crystallites. The resulting pale yellow solids were dried at 70°C under vacuum for 12 h. The remaining precursor ions in zeolite were removed by exchanging with aqueous 0.1 M $NaNO_3$ solutions. The stability of the encapsulated catalyst was checked after the reaction by UV–Vis and possible leaching of the complex was investigated by UV–Vis in the reaction solution after filtration of the zeolite. The amounts of Ni(II) complexes encapsulated in zeolite matrix were determined by elemental analysis and by subtracting the amount of Ni(II) complex left in the solutions after the synthesis as determined by UV–Vis spectroscopy.

2.10. *Oxidation of cyclohexene, general procedure*

In a typical reaction, 10 mL of cyclohexene and 1.2×10^{-5} mol of catalyst were added to a glass reactor with a gas inlet tube connected to a gas burette and an oxygen storage bottle. The mixture was heated to 70°C in a water bath and stirred with a magnetic stirring bar. The oxidation reactions were performed under atmospheric pressure of molecular oxygen in the absence of solvent; 2-cyclohexene-1-ol and 2-cyclohexene-1-one were the major products.

3. Results and discussion

3.1. *Synthesis and characterization*

The synthesis of $[Ni([R]_2\text{-}N_2X_2)]^{2+}$ ($R = H, CH_3$; $X = NH, O, S$) encapsulated in the nanopores of zeolite-Y was carried out by the flexible ligand method as described by Ratnasamy and co-workers [24]. The crude mass was subjected to Soxhlet extraction in methanol to remove excess ligand that remained uncomplexed in the nanocavities of the zeolite or located on the surface of the zeolite along with free $[Ni([R]_2\text{-}N_2X_2)]^{2+}$. The uncomplexed nickel(II) ions from the zeolite were removed by exchanging $[Ni([R]_2\text{-}N_2X_2)]^{2+}$–NaY with aqueous 0.01 M NaCl solution. Thus, presence of 0.638% of nickel(II) estimated by atomic absorption spectrometry is due only to encapsulation of the complex. The resulting catalyst was further characterized by recording its IR and electronic spectra and X-ray powder diffraction (vide infra) pattern. All these studies supported formation of $[Ni([R]_2\text{-}N_2X_2)]^{2+}$. Neat complexes have also been prepared by reaction of the 12-membered macrocyclic ligands (1,4-diaza, 7,10-dioxo, 5,6 : 11,12-dibenzo-[*e*, *k*]-cyclododeca-1,3-diene[N_2O_2]ane; $[H]_2$–N_2O_2, 2,3-dimethyl-1,4-diaza, 7,10-dioxo, 5,6 : 11,12-dibenzo-[*e*, *k*]-cyclododeca-1,3-diene[N_2O_2]ane; $[CH_3]_2$–N_2O_2, 1,4,7,10-tetraaza-5,6 : 11,12-dibenzo-[*e*, *k*]-cyclododeca-1,3-diene[N_4]ane; $[H]_2$–N_4, 2,3-dimethyl-1,4,7,10-tetraaza-5,6 : 11,12-dibenzo-[*e*, *k*]-cyclododeca-1,3-diene[N_4]ane; $[CH_3]_2$–N_4, 1,4-diaza, 7,10-dithia, 5,6 : 11,12-dibenzo-[*e*, *k*]-cyclododeca-1,3-diene [N_2S_2]ane; $[H]_2$–N_2S_2) and 2,3-dimethyl-1,4-diaza,7,10-dithia,5,6 : 11,12-dibenzo-[*e*, *k*]-cyclododeca-1,3-diene[N_2S_2]ane; $[CH_3]_2$–N_2S_2) in the presence of $LiClO_4$ with Ni(II) in refluxing methanol to yield the cationic complexes, $[Ni([R]_2\text{-}N_2X_2)](ClO_4)_2$, $R = H, CH_3$; $X = NH$, O, S (scheme 1). Acetonitrile solutions of these complexes were conductive (table 1). The molar conductance values of tetraaza macrocyclic complexes (239–263 $\Omega^{-1}\,mol^{-1}\,cm^2$) correspond to 1 : 2 electrolytes. Unfortunately, we could not grow single crystals suitable for X-ray crystallographic studies.

3.1.1. Chemical compositions of $[Ni([R]_2\text{-}N_2X_2)]^{2+}$ ($R = H, CH_3$; $X = NH, O, S$). The chemical compositions confirmed the purity and stoichiometry of the neat and encapsulated complexes. The chemical analysis of the samples revealed the presence of organic matter with a C/N ratio roughly similar to that for neat complexes. The nickel(II) ion contents estimated after encapsulation by AAS are only due to the presence of nickel(II) complexes in nanopores of zeolite-Y. The Si and Al contents in Ni(II)–NaY and the zeolite complexes are almost in the same ratio as in the parent zeolite, indicating little change in the zeolite framework due to dealumination in metal ion exchange. The parent NaY zeolite has Si/Al molar ratio of 2.53 which corresponds to a unit cell formula $Na_{56}[(AlO_2)_{56}(SiO_2)_{136}]$. The unit cell formula of metal-exchanged zeolites shows a nickel dispersion of 11.1 M per unit cell ($Na_{33.8}Ni_{11.1}[(AlO_2)_{56}(SiO_2)_{136}] \cdot nH_2O$). The analytical data of each complex indicates Ni : C : N molar ratios close to those calculated for the mononuclear structure. Elemental analysis and

Table 1. Elemental analysis and some physical properties for ligands and 12-membered macrocyclic nickel(II) complexes.

	Calculated (Found)							IR (KBr, cm^{-1})		
Complex	%C	%H	%N	C/N	%Ni	$\Lambda_M{}^a$, $\Omega^{-1} cm^2 moL^{-1}$	μ_{eff} (MB)	$\upsilon_{C=N}$	$\upsilon_{N–H}$	d↔d (nm)
$[H]_2–N_4$	72.70 (72.58)	6.10 (5.93)	21.20 (21.34)	3.43 (3.40)	–	–	–	1620	3310	–
$[CH_3]_2–N_4$	73.94 (73.79)	6.90 (6.79)	19.16 (19.28)	3.86 (3.83)	–	–	–	1618	3300	–
$[H]_2–N_2O_2$	72.16 (72.01)	5.30 (5.18)	10.52 (10.70)	6.86 (6.73)	–	–	–	1615	–	–
$[CH_3]_2–N_2O_2$	73.45 (73.28)	6.16 (6.04)	9.52 (9.66)	7.72 (7.59)	–	–	–	1613	–	–
$[H]_2–N_2S_2$	64.14 (64.00)	4.71 (4.59)	9.35 (9.50)	6.86 (6.74)	–	–	–	1605	–	–
$[CH_3]_2–N_2S_2$	65.98 (65.76)	5.54 (5.40)	8.55 (8.69)	7.72 (7.72)	–	–	–	1602	–	–
$[Ni([H]_2-N_4)](ClO_4)$	36.82 (36.60)	3.09 (2.92)	10.73 (10.90)	3.43 (3.36)	11.25 (11.13)	263		1600	3290	460
$[Ni([CH_3]_2-N_4)](ClO_4)$	39.31 (39.14)	3.67 (3.50)	10.19 (10.28)	3.86 (3.80)	10.67 (10.44)	255		1597	3285	465
$[Ni([H]_2-N_2O_2)](ClO_4)$	36.68 (36.42)	2.69 (2.50)	5.35 (5.48)	6.86 (6.65)	11.20 (11.11)	260		1595	–	463
$[Ni([CH_3]_2-N_2O_2)](ClO_4)$	39.17 (39.01)	3.29 (3.16)	5.07 (5.22)	7.72 (7.47)	10.63 (10.47)	253		1590	–	467
$[Ni([H]_2-N_2S_2)](ClO_4)$	34.49 (34.25)	2.53 (2.30)	5.03 (5.17)	6.86 (6.62)	10.53 (10.35)	250		1589	–	475
$[Ni([CH_3]_2-N_2S_2)](ClO_4)$	36.94 (36.73)	3.10 (2.94)	4.79 (4.88)	7.72 7.53)	10.03 (9.88)	239		1587	–	480

[a] In acetonitrile solutions.

spectroscopic data (tables 1 and 2) show that all of the neat complexes have tetrahedral structures.

3.1.2. IR spectral study. The absence of absorption at ca 3400 cm^{-1} in the IR spectra of ligands shows no free amino groups, and the absence of a strong band at ca 1670–1750 cm^{-1} shows the absence of ketonic groups, confirming elimination of water and cyclization to form the macrocyclic ligand. In the IR spectra of $[H]_2$–N_2O_2 and $[CH_3]_2$–N_2O_2 (~1620 cm^{-1}), $[H]_2$–N_4 and $[CH_3]_2$–N_4 (~1615 cm^{-1}) and $[H]_2$–N_2S_2 and $[CH_3]_2$–N_2S_2 (~1605 cm^{-1}), a new band appears in all the ligands corresponding to the υ(C=N) group. The IR spectra of these complexes show a moderate intensity absorption in the 1587–1600 cm^{-1} range attributed to the imine, υ(C=N) (table 1), shifted lower in the complexes, suggesting coordination through the nitrogen of (C=N). The spectra of ligands ($[H]_2$–N_4 and $[CH_3]_2$–N_4) show a band at ~3310 cm^{-1} corresponding to υ(N–H) [25]. On complexation, this band shifts to 3290 cm^{-1}, indicating diversion of the electron cloud from the nitrogen of the imidazole or amino group, thus resulting in a lowering of the N–H stretching frequency. IR spectra of the 12-membered macrocyclic ligands ($[R]_2$–N_2X_2) show bands in the 305–485 cm^{-1} range, which shift lower after complexation of the macrocyclic ligands [26].

The intensity of the peaks of encapsulated complex are weak due to low concentration of the complex in zeolite, but essentially similar to that of the free complex. However, significant changes in some important bands from the free ligand occur. For example, the free ligand exhibits ν(C=N) at 1580 cm^{-1}, while $[Ni([R]_2\text{-}N_2X_2)]^{2+}$–NaY and the neat complex display this band at 1540 and 1550 cm^{-1}, respectively. This shift indicates coordination of azomethine nitrogen to nickel. Appearance of three to four bands in the low frequency region 414–514 cm^{-1} suggests coordination of phenolic oxygen and in addition to azomethine nitrogen. The $[Ni([R]_2\text{-}N_2X_2)]^{2+}$–NaY exhibits bands at 1136, 1035, 960, 787 and 740 cm^{-1} due to the zeolite framework. No significant broadening or shift of the structure-sensitive zeolite vibration at 1130 cm^{-1} (due to asymmetric T–O stretch) on encapsulation indicates that there is no significant expansion of the zeolite cavity or dealumination during the encapsulation process. This further indicates that the metal complex fits nicely within the cavity of the zeolite. Thus, IR and UV–Vis data indicate the encapsulation of $[Ni([R]_2\text{-}N_2X_2)]^{2+}$–NaY in the zeolite nanocavity.

3.1.3. Diffuse reflectance spectra. The electronic spectra of Ni(II)–NaY do not show any absorption band above 300 nm, while spectra of $[Ni([R]_2\text{-}N_2X_2)]^{2+}$–NaY display one broad band at 315 nm, which is probably due to a symmetry forbidden ligand to metal charge transfer transition similar to that observed in nickel acetate [27] at 365 nm. The electronic spectra of $[Ni([R]_2\text{-}N_2X_2)]^{2+}$ exhibit one band at 465 nm which can be assigned to a d ↔ d transition of the metal ion. The average energy of this absorption is comparable to d ↔ d transitions of other square-planar Schiff-base nickel(II) chelates with nitrogen and oxygen donor atoms [27] (reported in the range of 460–480 nm). These data compare closely with the pure complex $[Ni([R]_2\text{-}N_2X_2)](ClO_4)_2$ as well as [Ni(salen)], indicative of a square-planer structure present in the nanocavity of the zeolite. The electronic spectral data of neat $[Ni([R]_2\text{-}N_2X_2)](ClO_4)_2$ and $[Ni([R]_2\text{-}N_2X_2)]^{2+}$–NaY are presented in tables 1 and 2. When the complexes were encapsulated in zeolite-Y, the d↔d band shifted again to higher energy (by ~3 nm). The stability of

Table 2. Chemical composition and IR stretching frequencies (as KBr pellets) of nanopores of zeolite encapsulated 12-membered macrocyclic nickel(II) complexes.

Sample	C (%)	H (%)	N (%)	C/N	Si (%)	Al (%)	Na (%)	Ni (%)	Si/Al	$\upsilon_{C=N}$ (cm^{-1})	d↔d (nm)
NaY	–	–	–	–	21.76	8.60	7.50	–	2.53	–	–
Ni(II)–NaY	–	–	–	–	21.79	8.49	3.28	3.72	2.53	–	–
$[Ni([H]_2-N_4)]^{2+}$–NaY	5.16	2.83	1.61	3.21	21.13	8.35	5.33	2.70	2.53	1598	457
$[Ni([CH_3]_2-N_4)]^{2+}$–NaY	5.23	2.89	1.49	3.50	21.08	8.33	5.30	2.69	2.53	1595	462
$[Ni([H]_2-N_2O_2)]^{2+}$–NaY	5.14	2.84	1.47	6.53	21.17	8.37	5.35	2.72	2.53	1593	461
$[Ni([CH_3]_2-N_2O_2)]^{2+}$–NaY	5.17	2.80	0.69	7.48	21.14	8.35	5.34	2.71	2.53	1585	464
$[Ni([H]_2-N_2S_2)]^{2+}$–NaY	5.09	2.77	0.78	6.55	21.09	8.33	5.29	2.68	2.53	1584	473
$[Ni([CH_3]_2-N_2S_2)]^{2+}$–NaY	5.12	2.82	0.69	7.45	21.02	8.31	5.28	2.64	2.53	1582	477

Table 3. Surface area and pore volume data of 12-membered macrocyclic nickel(II) complexes encapsulated in nanopores of zeolite Y.

Sample	Surface area ($m^2 g^{-1}$)[a]	Pore volume ($mL g^{-1}$)[b]
NaY	545	0.31
Ni(II)–NaY	532	0.30
$[Ni([H]_2-N_4)]^{2+}$–NaY	487	0.27
$[Ni([CH_3]_2-N_4)]^{2+}$–NaY	483	0.26
$[Ni([H]_2-N_2O_2)]^{2+}$–NaY	489	0.26
$[Ni([CH_3]_2-N_2O_2)]^{2+}$–NaY	488	0.25
$[Ni([H]_2-N_2S_2)]^{2+}$–NaY	479	0.25
$[Ni([CH_3]_2-N_2S_2)]^{2+}$–NaY	477	0.24

[a] Surface area is the "monolayer equivalent area" calculated as explained in references [22] and [23].
[b] Calculated by the *t*-method.

the complexes increases when they are encapsulated in zeolite-Y. The position of the d↔d band corresponds to a square-planar geometry for macrocyclic nickel(II) complexes [27].

3.1.4. X-ray diffraction. The X-ray powder diffractograms (XRD) of NaY, NiNaY and $[Ni([R]_2-N_2X_2)]^{2+}$–NaY were recorded to study crystallinity and to ensure encapsulation. An essentially similar pattern in Na–Y, metal ions exchanged zeolite and encapsulated metal complexes were observed with slight change in the intensity of the bands in encapsulated complexes. These observations indicate that the framework of the zeolite has not undergone any significant structural change during incorporation of the catalysts i.e. crystallinity of the zeolite-Y is preserved during encapsulation. Two new but weak peaks due to neat complexes were detected in the encapsulated zeolite at 2θ values of 1.74 and 8.22 due to loading of metal complexes. Encapsulation of the nickel complexes inside the zeolite nanocavities is indicated by the absence of extraneous material by scanning electron microscopy (SEM). Both X-ray diffraction and SEM indicated that zeolites with good crystallinity can be obtained during the encapsulation of nickel(II) complexes by the reaction.

3.1.5. Surface area and pore volume studies. The surface area and pore volume of the catalysts are shown in table 3. Inclusion of 12-membered macrocyclic nickel(II) complexes dramatically reduces the adsorption capacity and the surface area of the zeolite. It has been reported [28] that the BET surface area of X and Y zeolites containing phthalocyanine complexes are typically less than $100 m^2 g^{-1}$. The lowering of the nanopore volume and surface area indicate the presence of 12-membered macrocyclic nickel(II) complexes within the nanocavities of the zeolites and not on the surface.

3.2. *Catalytic activity*

The 12-membered macrocyclic nickel(II) complexes exhibited good activity in the oxidation of cyclohexene using molecular oxygen (table 4). Blank reactions performed over NaY zeolite under identical conditions show negligible conversion, indicating that

Table 4. Oxidation of cyclohexene with molecular oxygen catalyzed by "neat" azamacrocyclic nickel(II) complexes (reaction condition: 1 atm of O_2; time 8 h; catalyst 1.2×10^{-5} mol; substrate, cyclohexene 10 mL, temperature (70°C)).

		Selectivity (%)	
Catalyst	Conversion (%)	2-cyclohexene-1-ol	2-cyclohexene-1-one
$[Ni([H]_2\text{-}N_4)](ClO_4)$	67.5	70.3	29.7
$[Ni([H]_2\text{-}N_4)](ClO_4)^a$	45.1	79.7	20.3
$[Ni([H]_2\text{-}N_4)](ClO_4)^b$	60.7	64.5	35.5
$[Ni([H]_2\text{-}N_4)](ClO_4)^c$	38.9	56.7	43.3
$[Ni([CH_3]_2\text{-}N_4)](ClO_4)$	62.6	72.9	27.1
$[Ni([H]_2\text{-}N_2O_2)](ClO_4)$	60.3	65.8	34.2
$[Ni([CH_3]_2\text{-}N_2O_2)](ClO_4)$	55.9	68.4	31.6
$[Ni([H]_2\text{-}N_2S_2)](ClO_4)$	40.7	76.7	23.3
$[Ni([CH_3]_2\text{-}N_2S_2)](ClO_4)$	34.7	79.1	20.9

[a] Catalyst = 0.5×10^{-5} mol.
[b] Catalyst = 2.04×10^{-5} mol.
[c] Catalyst = 4.08×10^{-5} mol.

zeolite host is inactive for oxidation. Furthermore, O_2 alone is unable to oxidize the substrates in the absence of catalyst. In representative tests, zeolite complex was filtered out and the filtrate was analyzed for nickel content using atomic absorption spectrophotometry. The absence of nickel in solution phase indicates no leaching of complexes during reaction. These observations suggest that the oxidations occur due to the catalytic nature of the encapsulated 12-membered macrocyclic complexes and no significant role is played by either the zeolite support or free complexes.

2-Cyclohexene-1-ol is major product and 2-cyclohexene-1-one is formed in small quantities (table 4). Conversion for nickel(II) complexes with different macrocyclic ligands decreased in the order $[H]_2–N_4 > [CH_3]_2–N_4 > [H]_2–N_2O_2 > [CH_3]_2–N_2O_2 > [H]_2–N_2S_2 > [CH_3]_2–N_2S_2$ (for "neat" and encapsulated complexes) (tables 4 and 5). The encapsulated complexes exhibit higher activity than the "neat" complexes (figures 1 and 2).

$[Ni([H]_2\text{-}N_4)]^{2+}$–NaY complex has higher activity than other complexes [29]. Lower activity of $[Ni([CH_3]_2\text{-}N_4)]^{2+}$–NaY can be accounted for by the substantial steric hindrance of methyl groups that block the approaching oxidant.

Homogeneous catalysts are prone to deactivation by dimerization of active centers, which is expected to be reduced by encapsulating them in zeolites. $[Ni([H]_2–N_4)]^{2+}$–NaY was recycled for the oxidation of cyclohexene with molecular oxygen with a view to establish the effect of encapsulation on stability. The initial run showed conversion of 70.8% and it is only marginally reduced to 69.8% on recycling the catalyst (table 5), indicating that $[Ni([H]_2\text{-}N_4)]^{2+}$–NaY is stable to be recycled for oxidation of cyclohexene without loss in activity. Thus, encapsulation of complexes in zeolites increases the life of the catalyst by reducing dimerization. IR spectrum of the recycled sample is quite similar to that of fresh sample indicating little change after oxidation.

The results clearly suggest that $[Ni([H]_2\text{-}N_4)]^{2+}$–NaY efficiently catalyses conversion of cyclohexene to 2-cyclohexene-1-ol with 73.8% selectivity. More activity of the $[R]_2\text{-}N_2X_2$ system has clearly arisen from the existence of electron donating ligand, facilitating the electron transfer rate, a process previously observed by us in other oxidation reactions [30]. All conversions efficiencies obtained in this study are

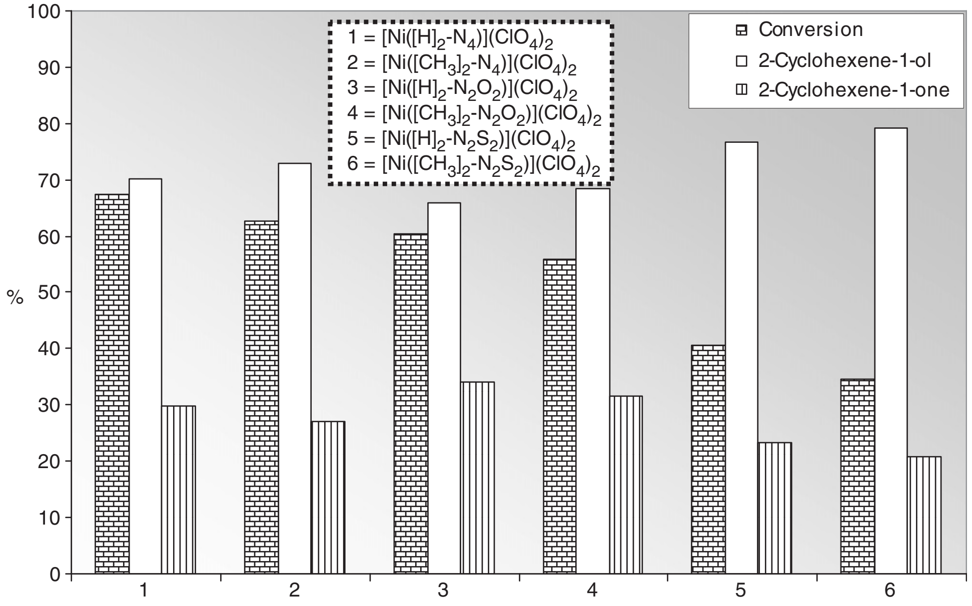

Figure 1. Bar diagram showing cyclohexene conversion and 2-cyclohexene-1-ol and 2-cyclohexene-1-one selectivity for various homogeneous catalysts.

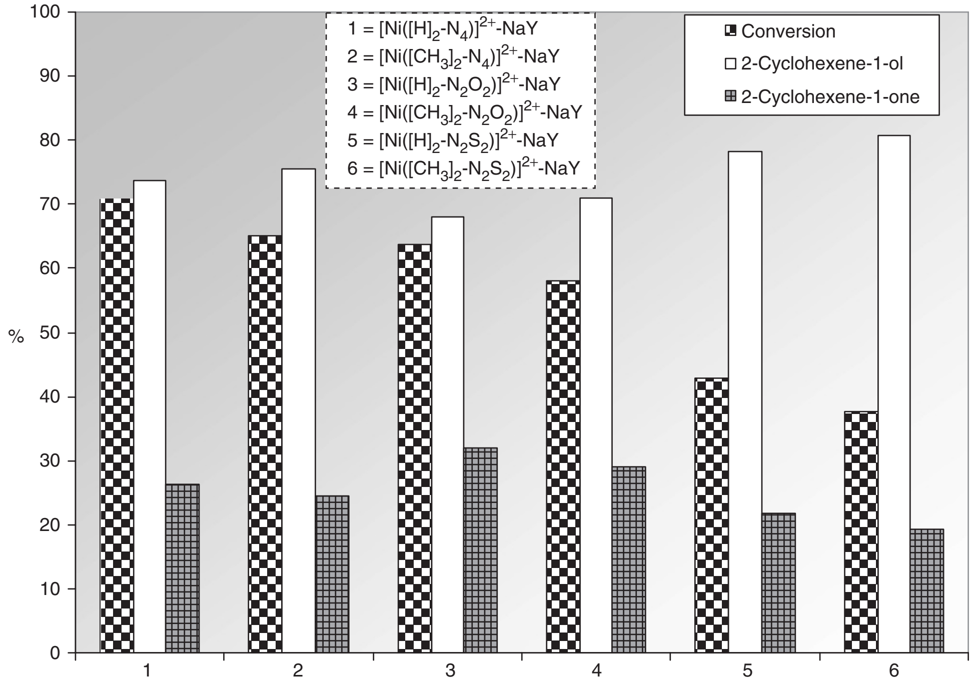

Figure 2. Bar diagram showing cyclohexene conversion and 2-cyclohexene-1-ol and 2-cyclohexene-1-one selectivity for various encapsulated catalysts.

Table 5. Oxidation of cyclohexene with molecular oxygen catalyzed by HGN (reaction condition: 1 atm of O_2; time 8 h; catalyst 1.2×10^{-5} mol; substrate, cyclohexene 10 mL).

Catalyst	Conversion (%)	Selectivity (%)	
		2-cyclohexene-1-ol	2-cyclohexene-1-one
$[Ni([H]_2\text{-}N_4)]^{2+}$–NaY	70.8	73.8	26.2
$[Ni([H]_2\text{-}N_4)]^{2+}$–NaY[a]	69.8	74.2	25.8
$[Ni([H]_2\text{-}N_4)]^{2+}$–NaY[b]	69.1	74.9	25.1
$[Ni([H]_2\text{-}N_4)]^{2+}$–NaY[c]	68.4	75.3	24.7
$[Ni([CH_3]_2\text{-}N_4)]^{2+}$–NaY	65.1	75.4	24.6
$[Ni([H]_2\text{-}N_2O_2)]^{2+}$–NaY	63.7	68.1	31.9
$[Ni([CH_3]_2\text{-}N_2O_2)]^{2+}$–NaY	58.1	70.9	29.1
$[Ni([H]_2\text{-}N_2S_2)]^{2+}$–NaY	42.9	78.2	21.8
$[Ni([CH_3]_2\text{-}N_2S_2)]^{2+}$–NaY	37.7	80.8	19.2

[a] First reuse.
[b] Second reuse.
[c] Third reuse.

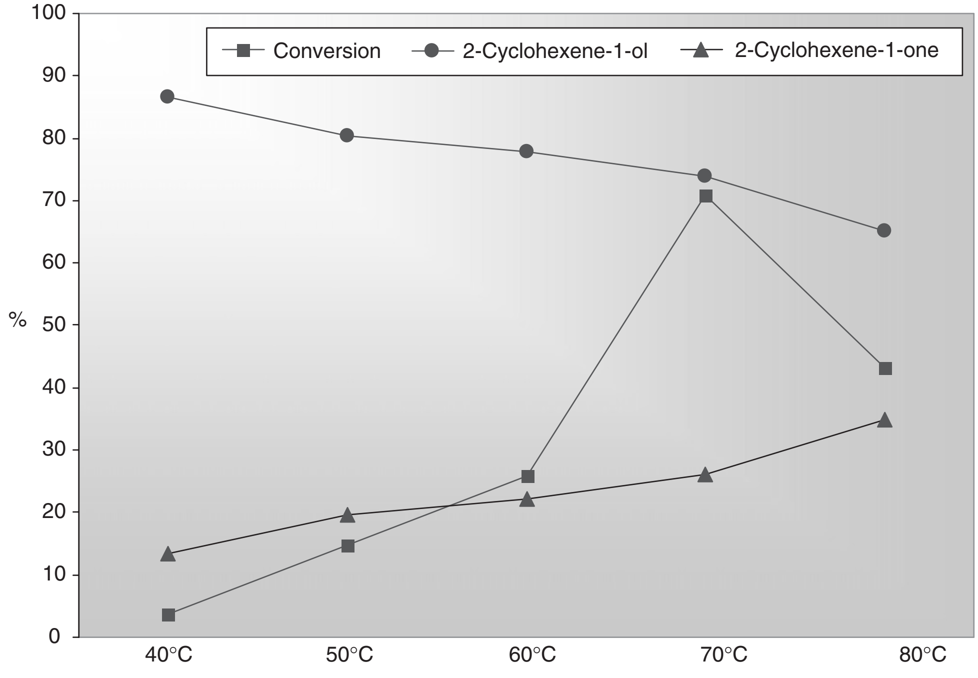

Figure 3. Diagram showing the effect of temperature on cyclohexene reactivity and product selectivity of $[Ni([H]_2\text{-}N_4)]^{2+}$–NaY.

significantly higher than those obtained using metal containing porous and nonporous materials [31, 32].

To investigate the effect of temperature on the reactivity and product selectivity of catalyst, oxidations were carried out only at temperatures from 40°C to 80°C for $[Ni([H]_2\text{-}N_4)]^{2+}$–NaY (figure 3). The reactivity and product selectivity of the complex varies with temperature. At 70°C the conversion is 70.8% and the selectivity to

2-cyclohexene-1-ol and 2-cyclohexene-2-one is 73.8% and 26.2%, respectively, while at 40°C, the conversion is 2.9% and the selectivity to 2-cyclohexen-1-ol and 2-cyclohexen-1-one is 86.4% and 12.1%, respectively. The reactivity is increased and selectivity to 2-cyclohexen-1-ol is decreased with increase in temperature.

4. Conclusions

The results show that the nickel(II) complexes with macrocyclic ligands were entrapped in the nanocavity of zeolite-Y by a two-step process in the liquid phase: (i) adsorption of precursor ligand, 1,2-di(*o*-aminophenyl-, amino, oxo, thio)ethane, N_2X_2, in the supercages of the Ni(II)–NaY, and (ii) *in situ* condensation of the Ni(II) precursor complex, $[Ni(N_2X_2)]^{2+}$, with glyoxal or biacetyl. The "neat" and zeolite-Y encapsulated nickel(II) macrocyclic complexes, $[Ni([R]_2\text{-}N_2X_2)]^{2+}$–NaY ($R = H, CH_3$; $X = NH, O, S$), exhibit catalytic activity in the oxidation of cyclohexene using O_2 with encapsulated complexes exhibiting enhanced activity and selectivity. These encapsulated systems offer structural integrity by having a uniform distribution of the metal complex in the nanopore structure of the support. The zeolite framework keeps the guest complexes dispersed and prevents their dimerization leading to the retention of catalytic activity. Future work on this system is expected for industrial applications for partial oxidation reactions.

Acknowledgement

Author is grateful to Council of University of Kashan for providing financial support to undertake this work.

References

[1] T. Joseph, D.P. Sawant, C.S. Gopinath, S.B. Halligudi. *J. Mol. Catal. A: Chem.*, **184**, 289 (2002).
[2] G.A. Somorjai, Y.G. Borodko. *Catal. Lett.*, **76**, 1 (2001).
[3] H.H. Kung, M.C. Kung. *Appl. Catal. A: Gen.*, **246**, 193 (2003).
[4] D. Kaucky, A. Vondrova, J. Dedecek, B. Wichterlova. *J. Catal.*, **194**, 318 (2000).
[5] (a) M. Hartman. *Angew. Chem. Int. Ed.*, **39**, 888 (2000); (b) A.G.F. Shoair, R.H. Mohamed. *J. Coord. Chem.*, **60**, 1279 (2007).
[6] M. Salavati-Niasari. *Inorg. Chem. Commun.*, **9**, 628 (2006).
[7] P. Chen, B. Fan, M. Song, C. Jin, J. Ma, R. Li. *Catal. Commun.*, **7**, 969 (2006).
[8] M. Salavati-Niasari, F. Davar. *Inorg. Chem. Commun.*, **9**, 263 (2006).
[9] A.G.F. Shoair. *J. Coord. Chem.*, **60**, 1101 (2007).
[10] R. Ferreira, M. Silva, C. Freire, B. de Castro, J.L. Figueiredo. *Microporous Mesoporous Mater.*, **38**, 391 (2000).
[11] S. Seelan, A.K. Sinha. *Appl. Catal. A: Gen.*, **238**, 201 (2003).
[12] V. Ayala, A. Corma, M. Iglesias, J.A. Rincón, F. Sánchez. *J. Catal.*, **224**, 170 (2004).
[13] K.M. Jinka, J. Sebastian, R.V. Jasra. *J. Mol. Catal. A: Chem.*, **274**, 33 (2007).
[14] M. Salavati-Niasari. *J. Mol. Catal. A: Chem.*, **217**, 87 (2004).
[15] M.R. Maurya, S.J.J. Titinchi, S. Chand. *J. Mol. Catal. A: Chem.*, **214**, 257 (2004).
[16] M.R. Maurya, S.J.J. Titinchi, S. Chand. *J. Mol. Catal. A: Chem.*, **201**, 119 (2003).
[17] P.P. Knops-Gerrits, D. Devos, F. Thibaultstarzyk, P.A. Jacobs. *Nature*, **369**, 543 (1994).

[18] I.W.C.E. Arends, R.A. Sheldon. *Appl. Catal. A: Gen.*, **212**, 175 (2001).

[19] P.P. Knops-Gerrits, F. Thibault-Starzyk, P.A. Jacobs. *Stud. Surf. Sci. Catal.*, **84**, 1411 (1994).

[20] K.J. Balkus, Jr, A.K. Khanrnamedova, K.M. Dixon, F. Bedioui. *Appl. Catal. A: Gen.*, **143**, 159 (1996).

[21] D. Chatterjee, A. Mitr. *J. Mol. Catal. A: Chem.*, **144**, 363 (1999).

[22] S.W. Wang, H. Everett, R.A.W. Haul, L. Moscou, R.A. Pierotti, J. Rouquerol, T. Siemieniewska. *Pure Appl. Chem.*, **57**, 603 (1985).

[23] A. Lineares-Solano. In *Textural Characterization of Porous Carbons by Physical Adsorption of Gases*. Carbon and Coal Gasification, J.L. Figueiredo, J.A. Moulijn (Eds), M. Nijhoff, M.A. Dordrecht, The Netherlands (1986).

[24] C.R. Jacob, S.P. Verkey, P. Ratnasamy. *Microporous Mesoporous Mater.*, **22**, 465 (1998).

[25] (a) P.K. Singh, J.K. Koacher, J.P. Tondan. *J. Inorg. Nucl. Chem.*, **43**, 1755 (1981); (b) M. Salavati-Niasari. *Micro. Meso. Mat.*, **92**, 173 (2006).

[26] M.R. Maurya, A.K. Chandrakar, S. Chand. *J. Mol. Catal. A: Chem.*, **270**, 225 (2007).

[27] K. Nakamoto. *Infrared and Raman Spectra of Inorganic and Coordination Compounds*, Wiley, New York (1978).

[28] (a) A.B. Lever. *Inorganic Electronic Spectroscopy*, 2nd Edn., Elsevier, New York (1968); (b) R.H. Holm, G.W. Evverett, A. Chakrvorty. *Prog. Inorg. Chem.*, **7**, 183 (1966); (c) M. Salavati-Niasari. *J. Mol. Catal. A: Chem.*, **283**, 120 (2008).

[29] K.J. Balkus, Jr, A.G. Gabrielov. *J. Inclusion Phen. Mol. Recognition Chem.*, **21**, 173 (1995).

[30] M. Silva, C. Freire, B. de Castro, J.L. Figueiredo. *J. Mol. Catal. A: Chem.*, **258**, 327 (2007).

[31] J.M. Thomas, R. Raja. *Chem. Commun.*, 675 (2001).

[32] J. Połtowicz, K. Pamin, E. Tabor, J. Haber, A. Adamski, Z. Sojka. *Appl. Catal. A: Gen.*, **299**, 235 (2006).

[33] M. Salavati-Niasari, A. Amiri. *Appl. Catal. A: Gen.*, **290**, 46 (2005).